

A Modeling and Simulation Approach for Reentry Vehicle Aeroshell Structural Assessment

David M. Kendall, Kaz Niemiec, and Richard A. Harrison

TRW Systems, Missile Defense Division

TRW led an Intercontinental Ballistic Missile Prime Integration Contract team in assessing the structural integrity of a reentry vehicle (RV) aeroshell to ensure that Air Force operational requirements would continue to be satisfied after modifications were made to the RV. As a result of the Comprehensive Test Ban Treaty, assessments of RVs necessarily rely significantly on analysis, primarily in the form of computer-based numerical simulations. Accurate structural response simulations of RVs require the integration of analyses from many different engineering disciplines. To have confidence in the simulations, the methodologies and models employed in each of these disciplines must be validated with test data. This paper presents the methods used for the RV aeroshell assessment as a case study to demonstrate how conventional testing methods, data from past nuclear environment simulation tests, and the integration of analyses from several engineering disciplines can be combined to perform high-fidelity simulations of RV responses to critical nuclear environments.

Introduction

Modifications to a reentry vehicle (RV) necessitated assessments of both the warhead and the RV aeroshell to ensure that Air Force operational requirements continue to be satisfied. Environments induced by nuclear events induce the highest stresses in the RV, and thus represent the critical load cases. Since the Comprehensive Test Ban Treaty prohibits underground and above-ground tests that simulate critical nuclear environment loadings, assessments of the RV rely heavily on analysis, primarily in the form of computer-based numerical simulations. Fortunately, technical advancements in both mathematical modeling of the RV physics and computational power have increased analysis fidelity. The continuation of these trends in technology suggests that, in the future, numerical simulations will be used almost exclusively in this arena. In particular, it is anticipated that future technical advancements will enable the analyses to continue to increase coupling and integration of classes of physics that have traditionally belonged to different engineering disciplines.

TRW led an Intercontinental Ballistic Missile Prime Integration Contract (IPIC) team in assessing the structural integrity of the RV aeroshell. Although the focus was on the evaluation of structural integrity, this effort required the contributions of many engineering disciplines as shown in Figure 1. This paper presents the methods used for the RV aeroshell assessment as a case study to demonstrate how conventional testing methods, data from past nuclear environment simulation tests, and the integration of analyses from many engineering disciplines can be combined to perform high fidelity simulations of RV responses to critical nuclear environments.

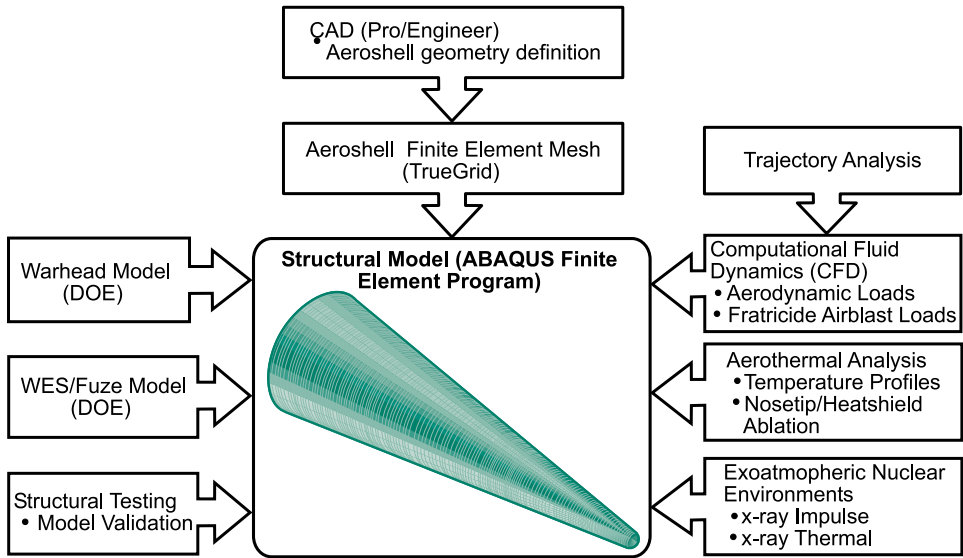


Figure 1. Engineering disciplines

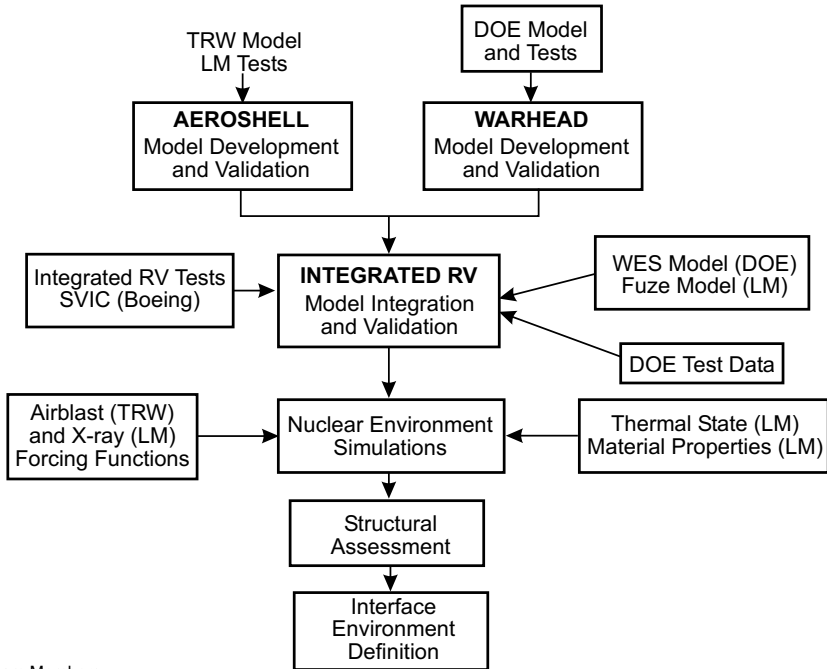
A comprehensive analysis and test program was defined and performed to develop validated analytical models and employ them to assess the RV structural integrity. Successful execution of the program required close cooperation between the IPIC team representing the U.S. Department of Defense, which has responsibility for the aeroshell, and the National Laboratories representing the Department of Energy (DOE), which has responsibility for the warhead and other internal components. The overall technical approach and the contributions of each team member are presented in Figure 2. The program consisted of three main elements:

1. *Model development.* Analytical models were developed to simulate structural responses of the RV subjected to nuclear environments. Specifically, TRW developed a finite element model of the aeroshell and the DOE teams provided finite element models of the warhead and the Warhead Electrical System (WES). Analytical models were also developed to derive flight and nuclear environmental data to serve as boundary conditions for the structural model.
2. *Model validation.* Extensive conventional structural dynamic testing was designed and performed with the primary purpose of developing data for validation of the structural model. Testing was performed at both component and system levels.
3. *Structural assessment.* The validated structural model was employed to simulate a number of critical loading events associated with nuclear encounters to assess structural integrity and define aeroshell/warhead interface environments.

These three main program elements—model development, model validation, and structural assessment—are described in detail below.

Model Development

The first element of the program was the development of analytical models to simulate the structural response under loading from critical nuclear environments. This effort involved not only the development of structural models, but also the development of models to



Team Members

- TRW
- Lockheed Martin Space Systems Company (LM), Valley Forge, Pa.
- Boeing, Survivability and Vulnerability Integration Center (SVIC), Ogden, Utah
- DOE National Laboratories

Figure 2. Technical approach and team members

derive flight and nuclear environmental data required as boundary conditions for the structural models. These environmental data included x-ray energy deposition impulse and thermal loads from exoatmospheric nuclear encounters, airblast loads from fratricide events, benign aerodynamic loading, nosetip and heatshield ablation states, and thermal profiles throughout the structure. To facilitate the integration of the analyses from the various engineering disciplines, we developed special-purpose software to map the data from all of these analyses into the structural model.

Structural Model Requirements. Before developing the aeroshell structural model, we reviewed aeroshell responses from past tests simulating nuclear environment loadings. In particular, a light-initiated high explosive (LIHE) test performed in the 1980s provided invaluable data for determining requirements for the model. In that test, an explosive material was sprayed on the outer surface of the aeroshell, and detonation was initiated by light. This test imparted an impulse load into the RV representative of an x-ray energy deposition. Several strain gauges were placed on the aeroshell and strain histories were successfully measured. These strain histories were analyzed for frequency content using a Lomb Periodogram.

Figure 3 presents four representative samples from the frequency content analyses—one hoop strain and one axial strain near the forward aeroshell/warhead interface, and one hoop strain and one axial strain near the aft aeroshell/warhead interface. Note that the first peak responses in the axial direction occur at a frequency of about 700 Hz and likely represent a high-order bending mode. The next peak responses occur near the forward support at a frequency of about 3300 Hz. Finally, a peak response in the hoop direction

near the aft support occurs at a frequency of about 4100 Hz. Thus, it was determined that the finite element model must be capable of accurately representing structural vibratory modes up to frequencies of at least 4100 Hz. This is a stringent requirement, since finite element models typically do well at capturing lower frequencies and tend to degrade in accuracy for higher frequency responses. A necessary condition for capturing high frequency responses is a refined finite element mesh capable of accurately representing high-order mode shapes.

Structural Model Development. The major components of the RV aeroshell include the nosetip, forward section, body section, antennas, and rear cover. These components were modeled in Pro/Engineer, a computer-aided design (CAD) program. The CAD models provided geometric definitions. The DOE uses a finite-element meshing program, TrueGrid, to develop their models. To provide a common platform for integrating their models, TrueGrid was selected for the aeroshell mesh development. The aeroshell model and the integrated RV model were analyzed with the commercial finite element program ABAQUS. The finite element model of the aeroshell is shown in Figure 4.

Both the forward and body sections consist of a tape-wound, carbon phenolic heatshield connected to an aluminum substructure via a soft bonding material layer. These components were modeled using continuum “brick” elements that incorporate additional incompatible displacement modes to improve bending response. The incompatible mode elements incorporate additional shape functions (and associated degrees of freedom) to eliminate artificial shear locking in bending. The additional shape functions are independent of adjacent elements, so the additional degrees of freedom can be condensed at the element level. Extensive numerical studies were performed to ensure that the continuum mesh with incompatible mode elements could adequately capture bending responses.

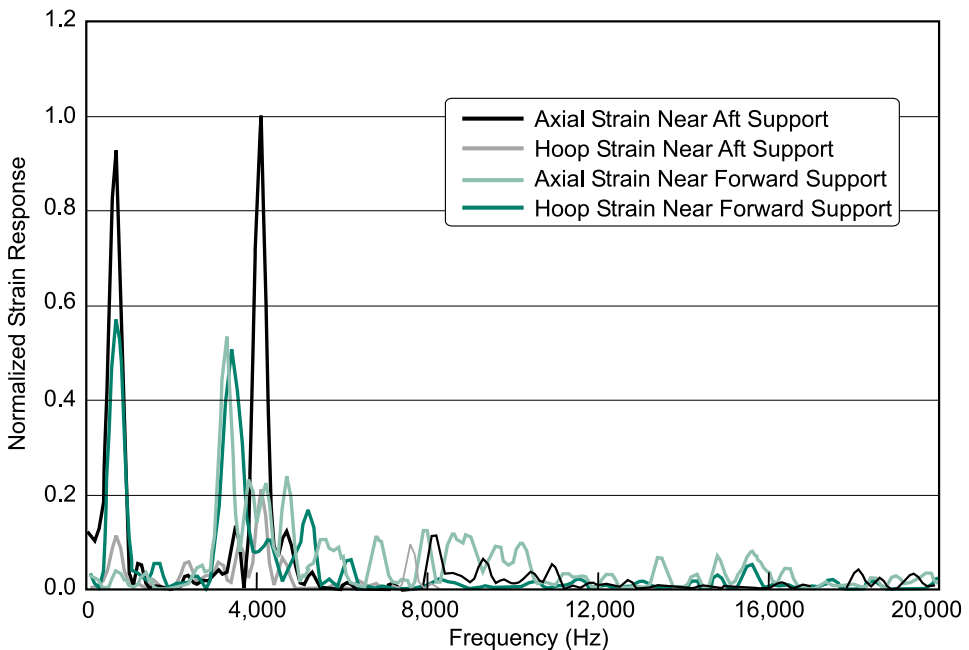


Figure 3. Lomb periodograms of LIHE test strain histories

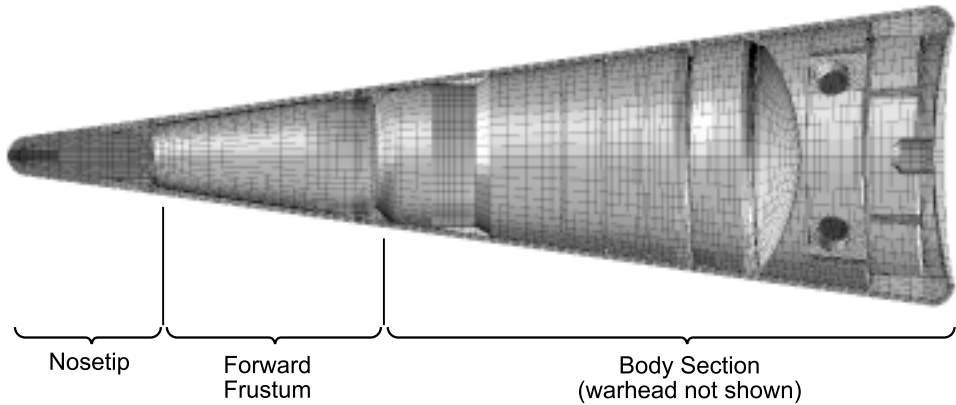


Figure 4. Aeroshell finite element model

The nosetip consists of a carbon-carbon composite with a tungsten composite insert for stability during shape change, and an aluminum cup at the base. Several variations of the nosetip and heatshield geometries were included in the TrueGrid model to represent different states of ablation corresponding to specific trajectory points of interest. The portion of the heatshield that was hotter than 1000°F was not included in the model since it contributes very little to stiffness or strength. However, the mass of the charred region was included. The heatshield and nosetip composite materials were modeled with temperature-dependent orthotropic constitutive models. The heatshield moduli and strength parameters are depicted in Figures 5 and 6, respectively.

The warhead model was supplied by the DOE teams in the form of TrueGrid files with geometric definitions, finite element mesh generation, and material properties. The warhead model also included the aft warhead attachment component and the forward support component. It is noted that the warhead model received by TRW, although comprehensive, was not nearly so refined as the model used internally by DOE in performing their analyses of the warhead. However, it was not necessary to employ an extremely detailed warhead model to assess aeroshell responses. In fact, TRW worked closely with the DOE teams to ensure that the warhead model employed for the aeroshell assessment had sufficient fidelity to accurately model the transmission of stresses from the aeroshell to the warhead, while keeping computational requirements to a tractable level.

The DOE teams also supplied the WES model. The Fuze was modeled by Lockheed Martin using lumped masses and user-defined stiffness matrices. TRW integrated these two models and then incorporated them into the aeroshell model.

The integrated RV model (aeroshell, warhead, WES, and Fuze) had about 800,000 degrees of freedom. Nonlinear interface behavior (contact) was modeled at the aeroshell/warhead interfaces.

Environmental Analyses. The employment of multiple RVs to attack single or nearby targets can lead to potential problems with fratricide. When the lead RV detonates, the ensuing blast wave propagates outward and can interact with the trailing RV. Transient (unsteady), three-dimensional, flow-field calculations were performed with an in-house computational fluid dynamics code to determine the temporal and spatial variations of the aeroshell surface pressure and shear stress caused by fratricidal airblast. A 6-degree-of-freedom algorithm was used to simulate the RV flight dynamics. The solution methodology employed two steps. First, calculations were performed to determine the steady-state

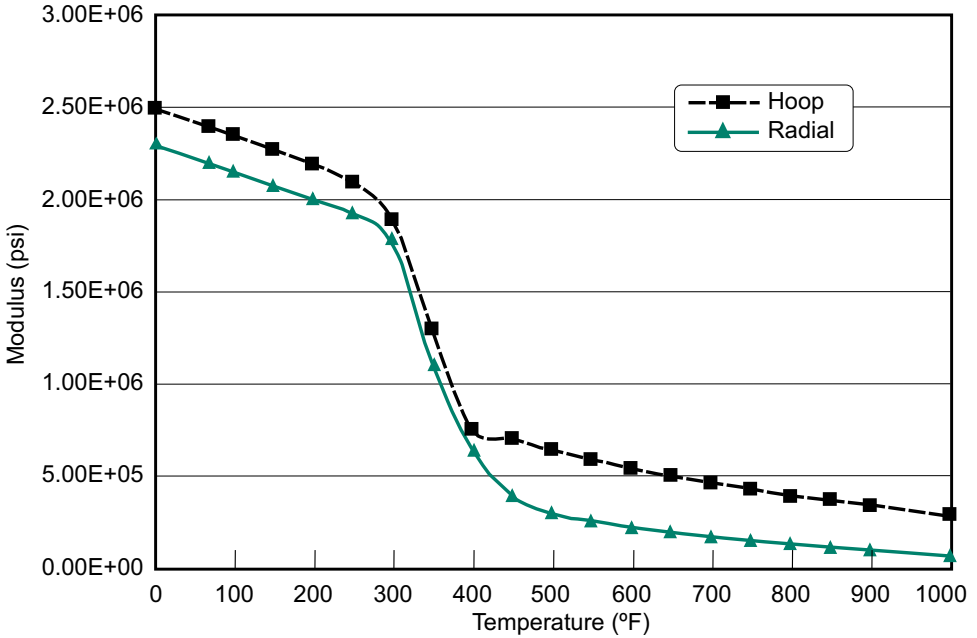


Figure 5. Temperature-dependent heatshield moduli

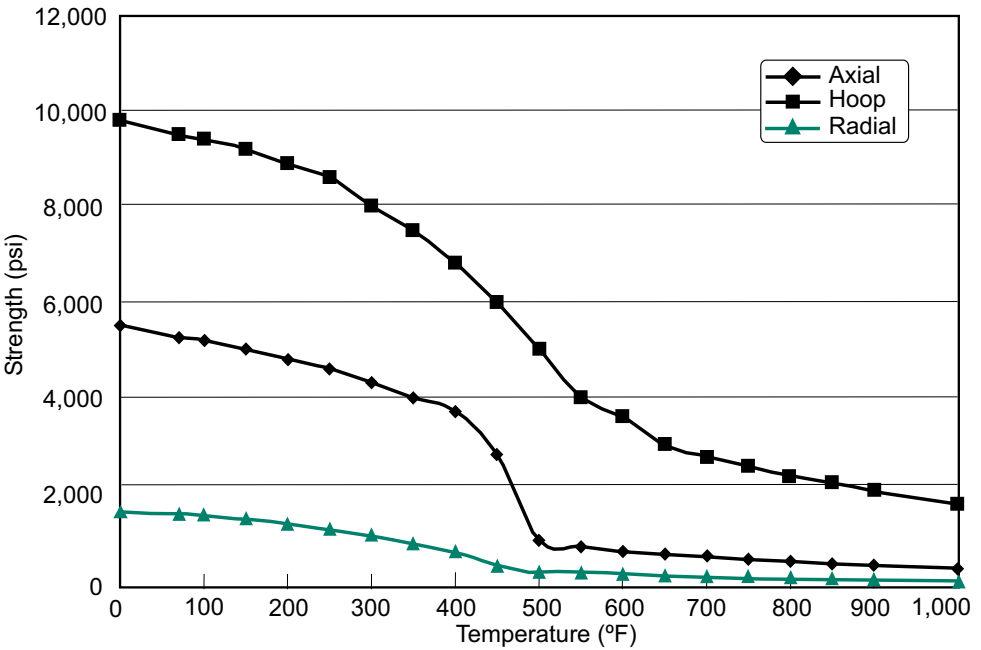


Figure 6. Temperature-dependent heatshield tensile strength

flow field around the RV just prior to the blast wave impingement on the vehicle. The RV Mach number and altitude were obtained from point-of-intercept calculations that involve analysis of the blast wave propagation, RV trajectory, and RV time-spacing requirements. Using the steady-state solution as initial conditions, a second analysis was performed to simulate the airblast encounter by flying the RV through the blast wave.

The analysis methodology used in the airblast predictions was validated by simulating an airblast test performed in the 1980s. In that test, a blast wave was generated by detonating an explosive in one end of a long pipe. An RV was suspended at the other end of the pipe, and thus was subjected to the generated pressure field. Analytical predictions correlated well with measured pressure data collected at several locations on the RV.

Aerothermal analyses were performed by Lockheed Martin to determine nosetip and heatshield ablation, as well as spatial variations in temperature, as a function of altitude for several different trajectories. In addition, thermal analyses were performed to determine temperatures resulting from exoatmospheric nuclear x-ray encounters along with the subsequent cooling during reentry to examine the effects of thermal preconditioning prior to fratricide airblast events. Lockheed Martin also derived environments caused by x-ray energy deposition during exoatmospheric nuclear encounters. The environments were defined for several blackbody temperatures with fluence levels based on weapons specifications.

Model Validation

The second element of the program was the design and performance of extensive conventional structural dynamic testing with the primary purpose of developing data for validation of the structural model. As described under Model Development, the models must be capable of accurately capturing responses with frequency content up to about 4100 Hz. This requirement on model fidelity translated to a need to gather data on the aeroshell up to the same frequency level.

Model validation is most efficiently and accurately performed first at the component level. Following that, system level model validation is necessary to characterize the interaction between components. In fact, for an RV, system-level testing is critical to determine the degree of load transfer between the aeroshell and the warhead. To this end, structural testing was performed both at the component level and at the system level.

To reduce time and expense, not every component of the aeroshell was tested. The critical aeroshell components with respect to structural response were judged to be the body section and the forward section, primarily because these two components have interfaces with the warhead. Since the forward and body sections use identical materials and fabrication processes, it was judged that testing of the body section would result in sufficient data to validate both components. Thus, structural testing was performed on the body section of the aeroshell.

Following that, an integrated test article designed as a high fidelity simulator of the complete RV underwent testing. This test article consisted of an aeroshell, a high-fidelity simulator of the warhead, a high-fidelity simulator of the WES, and a mass simulator of the Fuze. In addition to the tests performed by the IPIC team on these articles, the DOE teams supplied data on bending mode tests they performed on high-fidelity RV test articles. These tests provided additional data because the warhead attachment and support

conditions were varied to characterize the individual contributions of the attachment and support components. Each of the test series and their contribution to model validation is described below.

Aeroshell Body Section Modal Tests. The Lockheed Martin Space Systems Company performed the dynamic testing of the aeroshell body section. The first objective of the testing was to measure the mode shapes and natural frequencies for three selected vibratory shell modes. One mode was chosen for each of the low-, mid-, and high-frequency ranges. The number of longitudinal displacement waves (N) and the number of circumferential displacement waves (M) were the parameters used to define the shell modes. The approximate frequency of each of these modes was determined by exercising a pretest analytical model. The target modes are summarized in Table 1.

The second objective of the test was to measure structural dynamic impedance (drive point force and acceleration responses as a function of frequency) up to 5000 Hz at three locations where load transfer would occur between the aeroshell and the warhead in the RV. This objective was achieved by employing an electromechanical shaker device to impart a sinusoidal force through a “stinger” (connecting rod) at varying frequencies and measuring the acceleration at the loaded point. The locations and excitation are described in Table 2. The third objective of the testing was to measure structural damping for modes up to 5000 Hz.

Table 1. Aeroshell body section target mode characterization

Target Mode	Frequency (Hz)	Longitudinal Waves (N)	Circumferential Waves (M)
Low	400 to 500	0.5	3
Mid	2000 to 2500	0.5	7
High	3500 to 4000	1.0	9

Table 2. Aeroshell body section impedance tests

Location	Directly Loaded Component	Direction
Aft Payload Support	Heatshield	Radial
Aft Payload Support	Aluminum Substructure	Longitudinal
Forward Payload Support	Heatshield	Radial

As shown in Figure 7, the test article was suspended by bungee cords simulating “free-free” boundary conditions representative of flight conditions. Rigid body frequencies of the suspended test article were well below 10 Hz, indicating that the desired boundary conditions were accurately represented. The first accelerometer array used in testing included 108 accelerometers distributed in a pattern of 18 longitudinal by six circumferential. Longitudinally, the accelerometers were distributed over the length of the test article. Circumferentially, channels were placed every 30 deg over a 150-deg arc. Accelerations normal to the aeroshell were measured. This instrumentation set was used to characterize the low-frequency target mode shape, as well as characterization of damping.

As the frequency increases, the number of longitudinal and circumferential waves increases. Therefore, the mid- and high-frequency target modes were obtained using a second accelerometer array of 130 channels in a more closely spaced distribution on the surface of the aeroshell body. This array provided higher resolution over a more limited

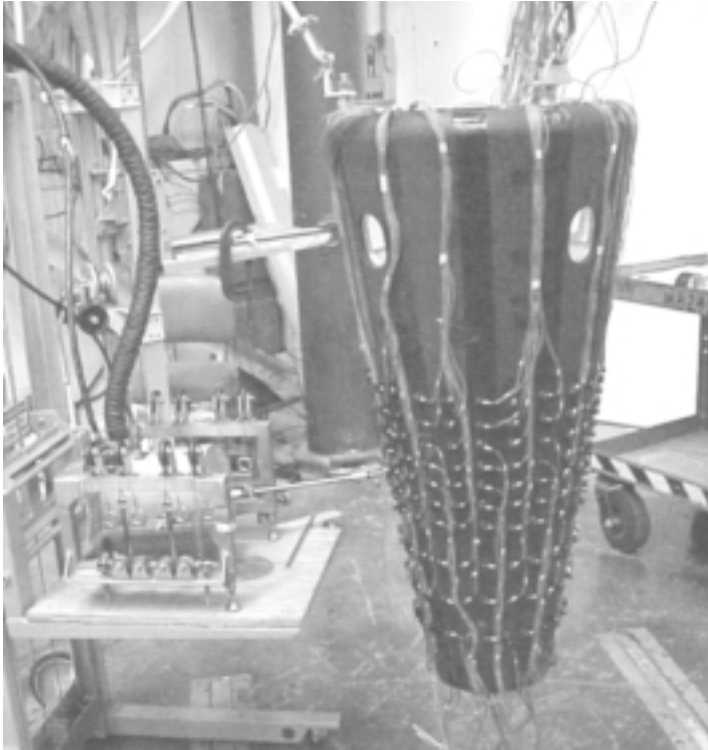


Figure 7. Aeroshell body section modal test setup

longitudinal span of the test article. Circumferential resolution was doubled to 15 deg over a 180-deg arc. The selection of 15-deg increments for circumferential accelerometer placement was based on a study of the aliasing effects of different array densities on shell mode shapes. This study took advantage of the known characteristics of the test article, such as symmetry, integer circumferential wave orders, and the drive point amplitude peak. The key result of the study was that the higher resolution array could capture mode shapes with circumferential wave numbers up to 12.

Concerns about the effects of the large number of accelerometers attached to the aeroshell on the measured frequencies motivated an additional test. After all test objectives were met, a final test was performed to determine the mass loading effect of the accelerometer array. All but eight of the 130 accelerometers were removed, and the previous test (that was performed with the full array of accelerometers) was repeated. A comparison of the two test runs indicated that the instrumentation mass resulted in an average decrease of natural frequency of 2.0% to 2.5%, with the greatest influence at higher frequencies. The test results were factored to account for this mass loading influence.

The analytical and measured frequencies for the target mode shapes are compared in Table 3. The measured frequencies are adjusted for instrumentation mass effects. The pretest predictions correlated well with test data; however, the model behavior was slightly softer than the test data over the range of measured frequencies. The model was adjusted by increasing the stiffness of the heatshield material by about 17% from our pretest prediction model. The heatshield properties were selected for adjustment because they had a larger material model uncertainty than the aluminum properties.

Table 3. Measured and analytical frequencies of target modes

Target Mode	Measured Frequency (Hz)	Pretest Analytical Prediction (Hz)	Adjusted Analytical Prediction (Hz)
Low	471	450	472
Mid	2247	2132	2240
High	3890	3727	3943

The measured and analytical mode shapes for the low-frequency target are compared in Figure 8 using normalized contour plots of displacement. Note that the two shapes are nearly identical. The mode shapes for the midfrequency target also showed excellent correlation. For the high-frequency mode shape, the measured data indicated that the N equals 1, M equals 9 mode shape was found at a frequency of 3890 Hz. However, the resulting contour plot did not appear to have enough data points to accurately represent the shape, and thus there was some uncertainty in the measured result.

After adjusting the model based on correlation with the target modes, the impedance tests were simulated analytically by integrating a model of the shaker mass and stinger into our body section model. Comparisons of analytical responses and measured responses were good for all the cases. A typical comparison of the spectral ratio of input acceleration to input force is plotted as a function of frequency in Figure 9.

Integrated RV Modal Testing. TRW and Boeing performed modal testing of a high-fidelity RV simulator at the Air Force Survivability and Vulnerability Center (SVIC) at Ogden, Utah. The first test objective was to characterize the bending modes of the RV under free-free boundary conditions. The second test objective was to measure the transmissibility of aeroshell shell modes across the interfaces to the warhead.

For the bending mode characterization, the test article was suspended vertically at the RV attachment bolts using bungee cords. The nosetip of the aeroshell was replaced with a hollow aluminum cylinder with mass properties equivalent to the real nosetip. The replacement nosetip provided an attachment point for the electromechanical shaker stinger and a conduit for instrumentation cables attached to instrumentation placed on internal components. Unfortunately, the test configuration significantly affected the measured results.

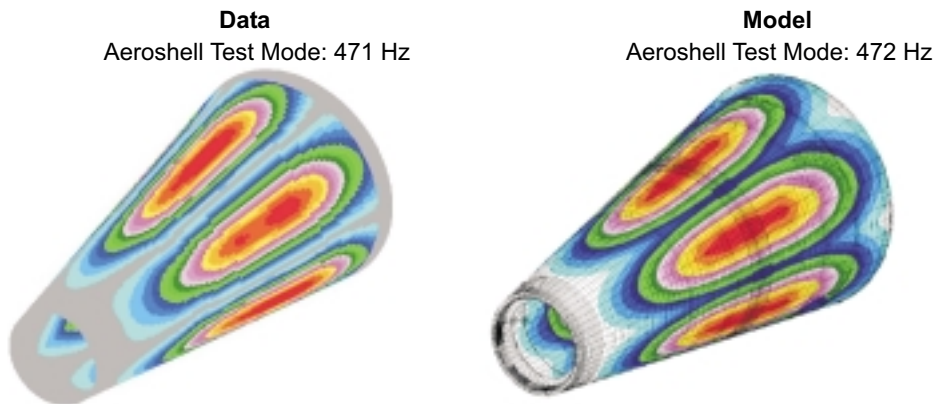


Figure 8. Low-frequency target mode shape comparison

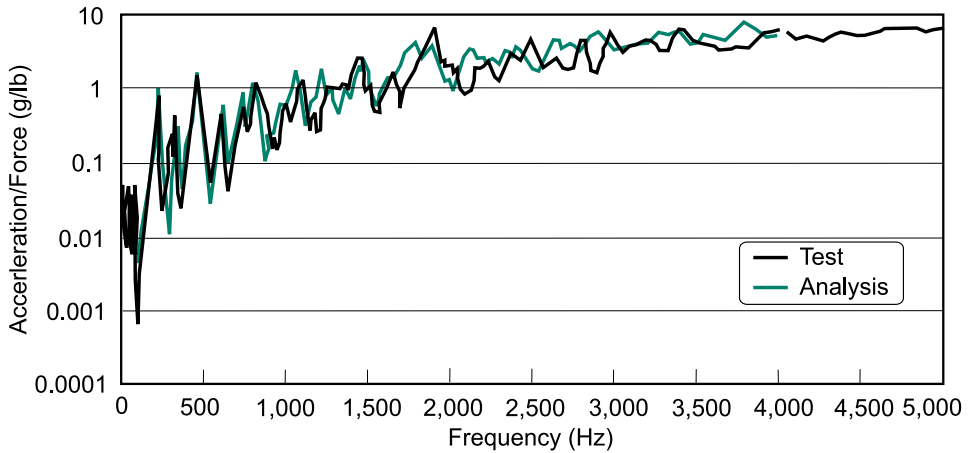


Figure 9. Radial admittance at aft payload support

To drive the system at high frequencies, the shaker/amplifier had to be set on the voltage control setting (versus the current control setting). This resulted in extremely high impedance at the shaker, essentially tying the RV nosetip to ground through the connecting rod for low-frequency RV responses. Thus, the low-frequency modes (below 300 Hz) did not have the appropriate boundary conditions. At higher frequencies, the mechanical impedance at the RV tip is much higher than that of the stinger, so the imposed boundary conditions were much closer to the free-free condition. Fortunately, test data from the DOE laboratories were available in the low-frequency range to supplement the usable high-frequency data obtained from the test. Furthermore, when the actual test conditions were simulated analytically (including the shaker and connecting rod), the model correlated well with the measured responses. A comparison of analytical and measured shapes of the fundamental bending mode is shown in Figure 10. A higher frequency mode shape is shown in Figure 11.

To characterize the transmissibility of aeroshell modes into the warhead, the aeroshell was excited by two opposing shakers, placed 180 deg apart. The shakers applied loads 180 deg out of phase so that the net applied lateral force on the article was zero. This was done with the goal of isolating shell mode responses from previously measured bending mode responses. The transmissibility was measured as the spectral ratio between the acceleration response in the warhead and the envelope of the spectrums of the aeroshell accelerometers. Although not shown here, the analytical results generally correlated well with the test data. The agreement in major response frequencies was within 8% with very similar amplitudes. However, based on the nosetip adapter accelerometer data, it appeared as though some bending modes were contributing to the measured responses, probably as a result of imperfections in the test loading conditions, which were not accounted for in the analytical model.

DOE Test Data. The DOE performed bending mode tests on a high-fidelity integrated RV test article suspended with bungee cords. An initial test was performed without the warhead forward support component to characterize bending modes with the warhead cantilevered from the aft payload support component. Data from this test were used to validate the analytical model of the aft payload support component. A second test was performed with the forward support component included. After validating the aft support

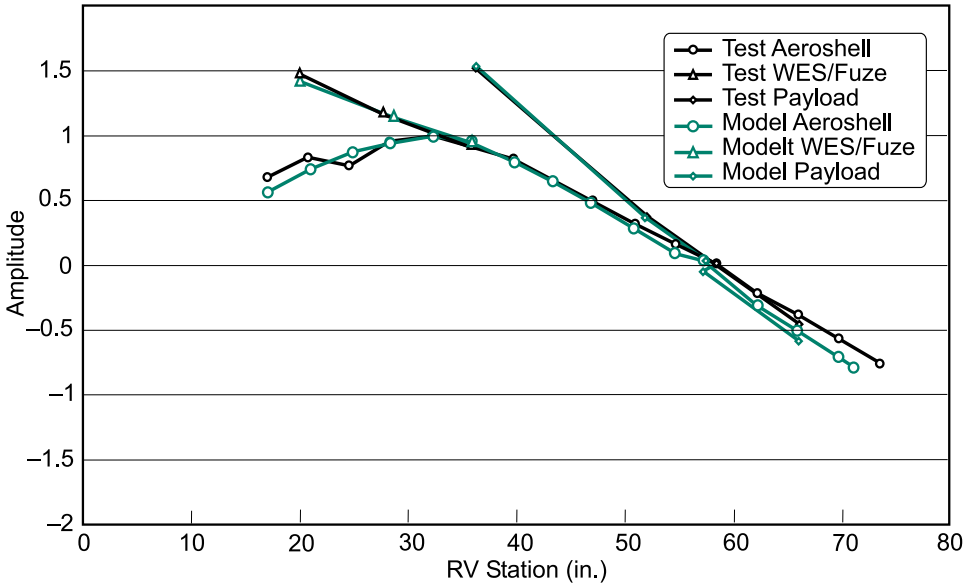


Figure 10. Fundamental bending mode shape

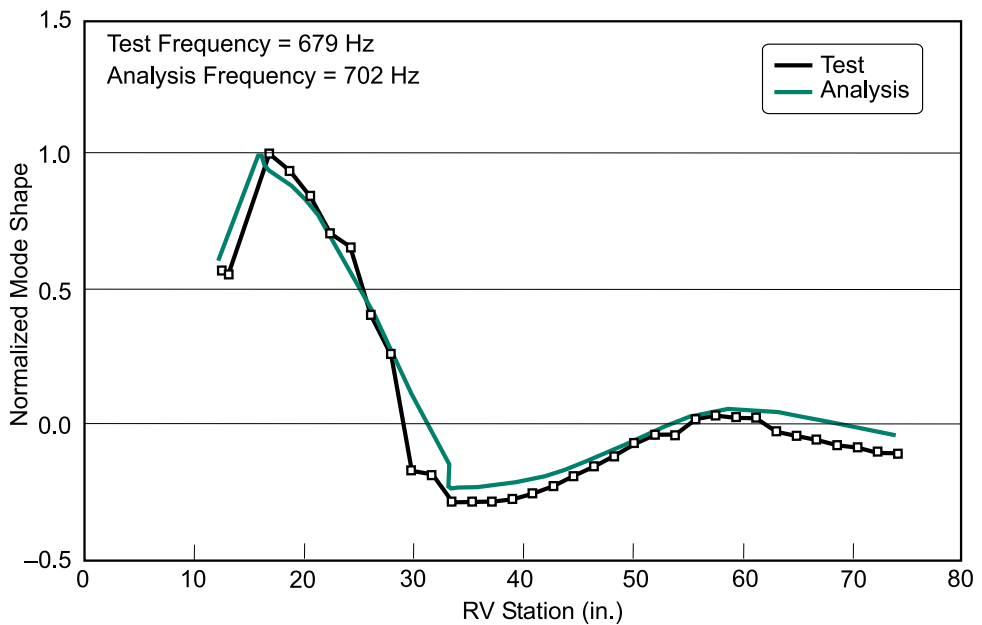


Figure 11. High-frequency bending mode shape

component model, the data from the second test were used to validate the forward support component. In addition, the test data supplemented the low-frequency data from the bending mode tests performed at SVIC.

LIHE Impulse Test Data. After validating the analytical model with conventional test data, the final validation step was performed by analytically simulating the LIHE test and comparing aeroshell strain history predictions with the measured data from that test. The

model slightly overpredicted the initial peak aeroshell strains near the forward support, but correlated well with initial peak aeroshell strains near the aft support. A comparison of the frequency content of the measured and analytical strain histories near the forward support is shown in Figure 12. Acceleration data from the test saturated early in the test event, but comparisons with the limited data showed that initial peak acceleration predictions at the aft warhead support correlated well.

The damping characteristics of the RV were obtained from both the integrated RV tests and the strain histories from the LIHE test. Damping characteristics are difficult to derive analytically, and thus test data are essential. To model nonlinear behavior of the RV analytically, a direct integration scheme was used to integrate the structural dynamic equations of motion. The primary disadvantage of this technique in comparison to modal decomposition schemes (which are best suited for linear responses) is that the damping matrix in ABAQUS is restricted to an algebraic combination of the mass matrix and stiffness matrix (Rayleigh damping). This type of damping has only the two parameters, and thus it is difficult to accurately capture the damping across the entire frequency range of interest. The two parameters were set to obtain the closest matches with both the first bending mode frequency and the high-frequency range (3300 to 4100 Hz), where the peak responses were demonstrated to be occurring.

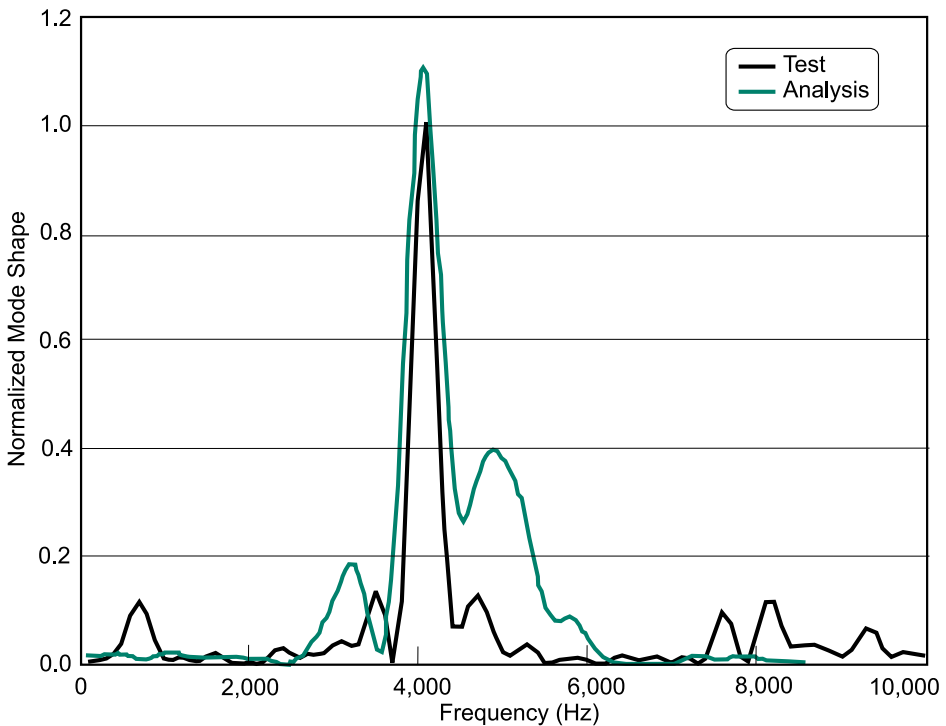


Figure 12. LIHE test strain comparison

Structural Assessment

The third element of the program involved applying the validated structural model to simulate a number of critical loading events associated with nuclear environment encounters and flight conditions. The specific cases analyzed are listed in Table 4, and are described below, along with the analytical methodology.

Table 4. Critical load case descriptions

Case	Loading Event	Loading Description	Trajectory	Thermal Preconditioning
1	Cold Blackbody temperature x-ray	Side-on impulse	Exoatmospheric	No
2	Medium Blackbody temperature x-ray	Thermal	Exoatmospheric	No
3	Hot Blackbody temperature x-ray	Internal impulse	Exoatmospheric	No
4	Fratricide airblast	Side-on pressure transient	V- γ point 1	No
5	Fratricide airblast	Side-on pressure transient	V- γ point 1	Previous fireball
6	Fratricide airblast	Head-on pressure transient	V- γ point 1	No
7	Fratricide airblast	Head-on pressure transient	V- γ point 1	Previous fireball
8	Fratricide airblast	Side-on pressure transient	V- γ point 2	No
9	Fratricide airblast	Side-on pressure transient	V- γ point 2	Previous fireball
10	Aerodynamic roll resonance	Steady-state aerodynamic	V- γ point 3	No
11	Aerodynamic roll resonance	Steady-state aerodynamic	V- γ point 3	X-ray thermal

X-ray Environment Load Cases. The first three cases listed in Table 4 pertain to environments from x-ray energy deposition with various blackbody temperatures. These environments result from exoatmospheric nuclear environments encounters. For the cold x-ray case, the energy is deposited in the outermost portion of the heatshield, and a small portion of the heatshield is vaporized, resulting in a “blow-off” impulse. A pressure transient applied to the external surface of the heatshield was employed to represent this impulse analytically.

For the medium blackbody temperature case, the x-rays pass through the heatshield and deposit energy on the aluminum substructure causing rapid heating of the aluminum. Thermal analyses were performed by Lockheed Martin to determine the spatial variation of peak temperatures throughout the aeroshell, and these temperatures were applied instantaneously to the structural model.

For the hot x-ray case, the x-rays pass through the aeroshell and deposit energy in the outermost portion of the warhead, resulting in material blow-off impulse. Pressure transients applied to both the external warhead and the internal aeroshell surfaces were employed to represent the resulting loads analytically.

The x-ray cases were analyzed using a structural model representing a virgin configuration; i.e., the nosetip and heatshield were not ablated and there was no aerodynamic heating of the structure. The virgin model was used because the x-ray events are exoatmospheric, and thus occur prior to reentry. Nonlinear, dynamic transient analyses were performed with an initial time step size on the order of 1 μ s. The time step size was gradually increased as the higher frequency responses became less dominant. Analyses were carried out to about 8 ms, which was more than sufficient to capture peak responses.

Reentry Airblast Load Cases. Cases 4 through 9 in Table 4 represent airblast load cases resulting from fratricide; i.e., an induced overpressure caused by a nuclear explosion from a lead RV interacting with a trailing RV. Each of these cases represents a different point on the V- γ map—a specific combination of RV velocity and angle-of-attack during reentry. In addition, both broadside and head-on impingement of the blast wave with the hypersonic RV were considered for some trajectories. Finally, each case was analyzed with and without a prior exoatmospheric nuclear encounter to assess the effects of thermal preconditioning of the structure. The load cases analyzed were chosen as potential worst-case conditions based on careful examination of trajectory analyses of vehicle axial and lateral accelerations, thermal analyses of ablation and structural temperatures, and multiple RV time spacing requirements.

For the airblast load cases, the geometry of the structural models was modified to account for both nosetip and heatshield ablation. The models also included prescribed thermal initial conditions to represent heating from reentry as well as heating from an exoatmospheric nuclear encounter.

The airblast load cases were analyzed using a combination of static and dynamic analyses. First, a nonlinear static analysis employing inertia relief was performed to simulate aerodynamic loading conditions just prior to blast-wave impingement. This technique uses mass proportional loading to balance the applied steady-state aerodynamic loads without requiring displacement boundary conditions to render the global stiffness matrix nonsingular. Following the static analysis, a nonlinear dynamic analysis was performed with the airblast pressure transients applied. The results of the prior static analysis were employed as initial conditions for the dynamic analysis. Based on an examination of the frequency content of the loading functions, an initial time step of 20 μ s was employed. Analyses were carried out to about 8 ms, which was more than sufficient to capture peak responses.

Roll Resonance Cases. The last two cases in Table 4 pertain to roll resonance, a phenomenon that occurs when the RV's roll rate is nearly equal to its characteristic pitch frequency. The near coincidence of these two frequencies results in an amplification of the trim angle of attack, and therefore potentially high lateral aerodynamic loads.

The first roll resonance typically occurs at high altitudes and is benign because the dynamic pressure is low and the RV is well balanced. However, there is a possibility that a second roll resonance can occur at a lower altitude. In this case, the dynamic pressure is high and the trim angle caused by ablation effects increased, so that lateral aerodynamic loads can be significant. The cases that were analyzed represent the maximum lateral loads ever expected as a result of second roll resonance, although the probability of occurrence is low.

Simulation Results. Following the simulation of each critical loading event, the generated structural response data were postprocessed using a computer program developed in-house to read through the ABAQUS output database, determine peak stress responses,

and compare them with temperature-dependent material allowable values. In addition, the dynamic responses were animated graphically to provide a visual means to assess the overall model behavior.

With the exception of one case, the structural response of the aeroshell was within allowable values. For the medium blackbody x-ray energy deposition case (the x-ray thermal loading case), the results indicated that some localized yielding would occur in the aluminum substructure. A thorough examination of the results and the applied temperatures led to the conclusion that the initial finite element model, presented earlier, did not have sufficient discretization to accurately model the steep temperature gradients in the aluminum or to capture the effects of localized material yielding. Thus, the model was refined by increasing the number of elements through the thickness of the aluminum substructure. To maintain accurate element aspect ratios, the number of elements around the circumference of the structure was also increased, resulting in a model with about 1.5 million degrees of freedom, representing a significant computational challenge. Furthermore, the aluminum material models were enhanced to include the effects of plastic material flow associated with yielding.

In addition, more refined thermal analyses were performed to generate the temporal variation of the peak temperatures, since it was reasoned that the steep gradients on the aluminum substructure would quickly equilibrate by thermal conductivity. An ABAQUS heat transfer model was created using the same mesh discretization as the structural model. A heat transfer analysis was performed to generate both spatial and temporal variations in temperature. The structural model was then reanalyzed using the results of the heat transfer analysis. Thus, the refined model had sufficient discretization, both in terms of the mesh and the forcing functions, to accurately model the structural response to the thermal loading. The final results indicated a very small region with yielding that would not cause structural failure.

Based on the results of all the load cases, the assessment demonstrated that the RV aeroshell is structurally robust and continues to meet Air Force operational requirements for both structural integrity and aeroshell/warhead interface environments.

Summary

The Comprehensive Test Ban Treaty and recent technology advancements suggest that the design and verification of RVs will rely heavily on analytical simulations, particularly in the area of nuclear environment survivability. Based on the work described in this paper, as well as analytical efforts performed at the DOE National Laboratories, it appears that the confidence placed on modern simulation tools is warranted. However, successful simulations require the integration of analyses from many different engineering disciplines, and thus many different complementary analytical tools are required. The methodologies and models employed in each of the disciplines must be validated with test data. In the absence of underground and above-ground tests simulating critical nuclear environments loading, test data must be obtained by more conventional means such as material characterization tests, structural dynamic tests at both component and system levels, or ablation data from flight tests. Data from previous nuclear environment tests are a valuable source for validating methods, even if applied to a different or modified RV.



David M. Kendall is a TRW Systems Technical Fellow and performs structural analysis for the Propulsion, Structures and Fluid Mechanics Department of the TRW Missile Defense Division, San Bernardino, California. He has worked for TRW for 18 years developing finite element technology and applying it to a variety of structures including launch vehicles, targets, and reentry vehicles, and missile silos. He has published several papers in technical journals and conference proceedings. He holds a BS and an MS in civil engineering from the University of California at Davis, and earned a PhD in applied mechanics from the University of California at San Diego.

dave.kendall@trw.com



Kaz Niemiec is a senior engineer with the Propulsion, Structures and Fluid Mechanics Department of the TRW Missile Defense Division, San Bernardino, California. He has 22 years of experience at TRW in missile and launch vehicle structures, structural dynamic modeling, loads, dynamics, shock, vibration, acoustic design, analyses, requirements, and test. He has held technical leadership positions for Minuteman, Peacekeeper, SICBM, reentry vehicles, and various target launch vehicles. He has 32 years of experience in dynamics, shock, vibration and acoustic design, analysis and test, including automotive, ship silencing, missiles and launch vehicles and payloads. He holds a BS in mechanical engineering from the University of California at Los Angeles.

kaz.niemiec@trw.com



Richard A. Harrison has been with TRW for 18 years. He is currently a senior engineer performing structural analysis with the Propulsion, Structures, and Fluid Mechanics Department in the TRW Missile Defense Division. Previous endeavors within TRW have included medical equipment design for which he holds a patent, and IR&D lead on environmental engineering. He presented a paper on lunar habitat development at a NASA conference. Prior to joining TRW he was a structural engineer in both the petrochemical and architectural industries. He received a BS in civil engineering and an MS in structural engineering from the University of California at Davis.

richard.harrison@trw.com